

Preparation and Structural Characterization of the Palladium(0)–Carbonyl Complexes $(R_2PC_2H_4PR_2)Pd(CO)_2$ and $\{(R_2PC_2H_4PR_2)Pd\}_2(\mu-CO)^\dagger$

Roman Trebbe, Richard Goddard, Anna Ruffńska, Klaus Seevogel, and Klaus-Richard Pörschke*

Max-Planck-Institut für Kohlenforschung, Postfach 10 13 53,
D-45466 Mülheim an der Ruhr, Germany

Received April 6, 1999

$(d^i\text{ppe})Pd(C_2H_4)$ and $(d^t\text{bpe})Pd(C_2H_4)$ react with an excess of CO to afford the novel tetrahedral Pd^0 –dicarbonyl complexes $(d^i\text{ppe})Pd(CO)_2$ (**1**) and $(d^t\text{bpe})Pd(CO)_2$ (**2**). Partial CO elimination from **2** yields dinuclear $\{(d^t\text{bpe})Pd\}_2(\mu-CO)$ (**3**), containing a single bridging carbonyl ligand. **3** represents the smallest cluster containing the $Pd_2(\mu-CO)$ group and, as such, is also the simplest model compound for CO adsorption on a Pd(100) surface. Thermolysis of **3** produces a carbonyl-free product which is assumed to be the dinuclear species $\{(d^t\text{bpe})Pd\}_2$ (**4**). The molecular structures of **2** and **3** have been determined, and the solids are furthermore characterized by CP-MAS NMR spectra.

Introduction

Isolated mononuclear Pd^0 –carbonyl complexes are rare. Examples include $(Ph_3P)_3Pd(CO)$, which on reversible phosphine dissociation gives rise to $(Ph_3P)_2Pd(CO)$, which itself has not been isolated,^{1a} $\{N(C_2H_4PPh_2)_3\}Pd(CO)$,^{1b} and $\{MeC(CH_2PPh_2)_3\}Pd(CO)$,^{1c} the last compound has been structurally characterized. Matrix isolation techniques have allowed the spectroscopic characterization of the highly unstable homoleptic complexes $Pd(CO)_n$ ($n = 1-4$).² Nevertheless, until now, no stable Pd^0 –dicarbonyl complex $L_nPd(CO)_2$ has been prepared.

The dinuclear Pd^0 –carbonyl complexes $\{(bpy)Pd(\mu-CO)\}_2$ and $\{(o\text{-phen})Pd(\mu-CO)\}_2$ ³ and trinuclear clusters $L_nPd_3(CO)_3$ ($L = PPh_3$; $n = 3, 4$;^{1a} $L = P^tBu_3$, PPh^tBu_2 ; $n = 3$)⁴ have been reported, but without structural data. The molecular structures of larger clusters such as $(Ph_2MeP)_4Pd_4(\mu_2-CO)_5$,^{5a} $(nBu_3P)_4Pd_4(\mu_2-CO)_6$,^{5b} $(Me_3P)_7Pd_6$ –

$(\mu_3-CO)_4$,^{5c} and $(Me_3P)_7Pd_7(\mu_2-CO)_3(\mu_3-CO)_4$ ^{5d} have, however, been established.⁶ Dinuclear $Pd_2(\mu-CO)$ bonding has been suggested for adsorption of CO on a Pd(100) surface,⁷ but interestingly no examples of dinuclear Pd^0 –monocarbonyl complexes are known.

Here we report the synthesis and properties of the novel mononuclear complexes $(R_2PC_2H_4PR_2)Pd(CO)_2$ ($R = ^iPr$ (**1**), tBu (**2**)), with terminal CO ligands, and the dinuclear $\{(d^t\text{bpe})Pd\}_2(\mu-CO)$ (**3**), containing a single CO bridge.⁸

Results and Discussion

$(d^i\text{ppe})Pd(CO)_2$ (1) and $(d^t\text{bpe})Pd(CO)_2$ (2). When colorless pentane solutions of $(d^i\text{ppe})Pd(C_2H_4)$ and $(d^t\text{bpe})Pd(C_2H_4)$ ⁹ are treated with an excess of CO at ambient temperature, the solutions first turn red (presumably due to the intermediate formation of complexes of type **3**) and then decolorize again. At $-78^\circ C$ colorless crystals of the Pd^0 –dicarbonyl complexes **1** and **2** separate in 70–80% yield (Scheme 1). The syntheses represent equilibrium reactions. Thus, when ethene is bubbled into solutions of **1** and **2** the starting Pd^0 –ethene complexes are recovered. The solid $d^i\text{ppe}$ complex **1** decomposes at $42^\circ C$, whereas the sterically more encumbered $d^t\text{bpe}$ derivative **2** is stable to $125^\circ C$. Thermolysis presumably proceeds by partial or complete

[†] Abbreviations: bpy, 2,2'-bipyridyl; $d^i\text{ppe}$, bis(diisopropylphosphino)ethane, $\{R_2PC_2H_4P^iPr_2\}$; $d^t\text{bpe}$, bis(di-*tert*-butylphosphino)ethane, $\{Bu_2PC_2H_4P^tBu_2\}$; DTA, differential thermal analysis; FIR, far-infrared; *o*-phen, 1,10-phenanthroline.

(1) (a) Misono, A.; Uchida, Y.; Hidai, M.; Kudo, K. *J. Organomet. Chem.* **1969**, *20*, 7. Kudo, K.; Hidai, M.; Uchida, Y. *J. Organomet. Chem.* **1971**, *31*, 393. Morandini, F.; Consiglio, G.; Wenzinger, F. *Helv. Chim. Acta* **1979**, *62*, 59. (b) Ceconi, F.; Ghilardi, C. A.; Midollini, S.; Moneti, S.; Orlandini, A.; Scapacci, G. *J. Chem. Soc., Dalton Trans.* **1989**, 211. (c) Grévin, J.; Kalck, Ph.; Daran, J. C.; Vaissermann, J.; Bianchini, C. *Inorg. Chem.* **1993**, *32*, 4965.

(2) Darling, J. H.; Ogden, J. S. *Inorg. Chem.* **1972**, *11*, 666; *J. Chem. Soc., Dalton Trans.* **1973**, 1079. Huber, H.; Kündig, P.; Moskovits, M.; Ozin, G. A. *Nature, Phys. Sci.* **1972**, *235*, 98.

(3) Burianová, J.; Burianec, Z. *Collect. Czech. Chem. Commun.* **1963**, *28*, 2138. In light of our results a reinvestigation of these products appears desirable.

(4) Yoshida, T.; Otsuka, S. *J. Am. Chem. Soc.* **1977**, *99*, 2134.

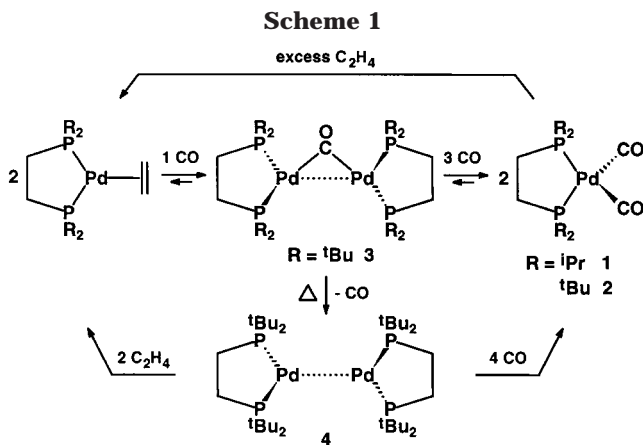
(5) (a) Dubrawski, J.; Krieger-Simonsen, J. C.; Feltham, R. D. *J. Am. Chem. Soc.* **1980**, *102*, 2089. (b) Mednikov, E. G.; Eremenko, N. K.; Mikhailov, V. A.; Gubin, S. P.; Slovokhotov, Y. L.; Struchkov, Y. T. *J. Chem. Soc., Chem. Commun.* **1981**, 989. Mednikov, E. G.; Eremenko, N. K.; Gubin, S. P.; Slovokhotov, Y. L.; Struchkov, Y. T. *J. Organomet. Chem.* **1982**, *239*, 401. (c) Klein, H.-F.; Mager, M.; Flörke, U.; Haupt, H.-J. *Organometallics* **1992**, *11*, 3915. (d) Goddard, R.; Jolly, P. W.; Krüger, C.; Schick, K.-P.; Wilke, G. *Organometallics* **1982**, *1*, 1709.

(6) The largest structurally characterized Pd^0 –CO cluster so far is $(Me_3P)_{21}Pd_{59}(CO)_{32}$: Tran, N. T.; Kawano, M.; Powell, D. R.; Dahl, L. F. *J. Am. Chem. Soc.* **1998**, *120*, 10986. For clusters of intermediate size see references therein.

(7) (a) Bradshaw, A. M.; Hoffmann, F. M. *Surf. Sci.* **1978**, *72*, 513. Ortega, A.; Hoffmann, F. M.; Bradshaw, A. M. *Surf. Sci.* **1982**, *119*, 79. (b) Behm, R. J.; Christmann, K.; Ertl, G.; Van Hove, M. A.; Thiel, P. A.; Weinberg, W. H. *Surf. Sci.* **1979**, *88*, L59. Behm, R. J.; Christmann, K.; Ertl, G.; Van Hove, M. A. *J. Chem. Phys.* **1980**, *73*, 2984.

(8) Trebbe, R. Dissertation, University of Düsseldorf, Germany, 1999.

(9) Krause, J.; Bonrath, W.; Pörschke, K.-R. *Organometallics* **1992**, *11*, 1158.



cleavage of the CO ligands. Although the IR carbonyl stretching bands of the solids (KBr) are somewhat broad, attributable to packing effects, the spectra observed for pentane solutions are sharply resolved and indicative of terminally coordinated CO ligands. For **2** the Pd⁰–CO bands are at 2012 (A₁) and 1969 (B₁) cm⁻¹ and thus lie at higher wavenumbers than those of the homologue (d⁴bpe)Ni(CO)₂ (1994 and 1935 cm⁻¹),¹⁰ in agreement with the common wisdom that back-bonding is weaker for Pd⁰ than for Ni⁰. In the solution ¹³C NMR spectra (27 °C) of **1** and **2** the CO ligand gives rise to a signal at $\delta(C)$ 199, which at -80 °C is split into a narrow triplet ($^2J(PC) \approx 4$ Hz). The temperature dependence of the spectra suggests a reversible cleavage of a CO ligand in solution. For comparison, for (Ph₃P)₃Pd(CO) $\nu(CO)$ is at 1957 cm⁻¹ and the NMR resonance of the CO ligand (-70 °C) is a quartet at $\delta(C)$ 197 ($^2J(PC) \approx 6$ Hz).^{1a}

Similar to what is found for (d¹ppe)Pd(C₂H₄) and (d⁴bpe)Pd(C₂H₄),⁹ the Pd⁰–carbonyl complexes **1** and **2** react with ethyne by displacement of the CO ligands to produce (d¹ppe)Pd(C₂H₂) and (d⁴bpe)Pd(C₂H₂). Thus, while the *ethene* ligands in the starting L₂Pd(C₂H₄) complexes and the *carbonyl* ligands in the corresponding L₂Pd(CO)₂ complexes **1** and **2** can be mutually displaced by CO and ethene in equilibrium reactions, both ligands are displaced by *ethyne* to give L₂Pd(C₂H₂) complexes, allowing an assessment of the relative thermodynamic stabilities.

Molecular Structure of 2. The molecular structure of **2** (Figure 1) has been determined by X-ray crystallography. Despite different environments, the two independent molecules in the asymmetric unit are identical within experimental error. The Pd atom is tetrahedrally coordinated by the d⁴bpe P atoms and two terminally bound carbonyl ligands. The bite angle of the chelating d⁴bpe ligand at 88.1(2)° (mean) is similar to that in other TP-3 (R₂PC₂H₄PR₂)Pd⁰ complexes,^{11,12} while the OC–Pd–CO angle of 110.2(7)° (mean) corresponds to that of an ideal tetrahedron. The Pd–P bond lengths of 2.408(5) Å (mean) in T-4 **2** are significantly

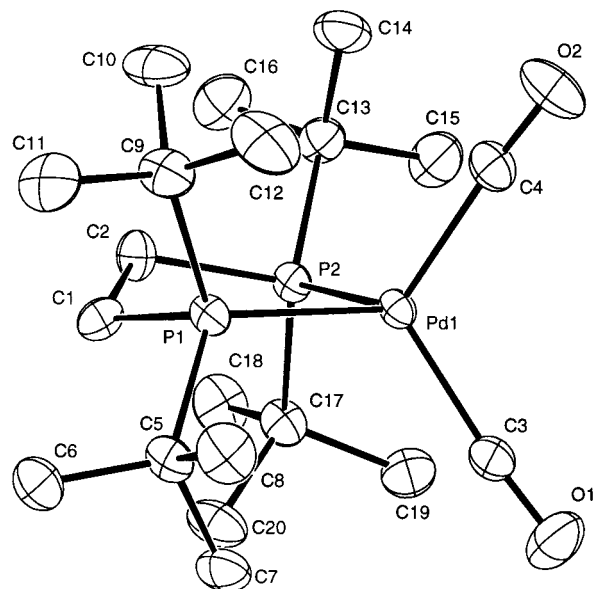


Figure 1. Molecular structure of one of the independent molecules of complex **2**. Selected bond distances (Å) and angles and dihedral angles (deg) of molecule 1: Pd1–P1 = 2.404(1), Pd1–P2 = 2.405(1), Pd1–C3 = 1.940(3), Pd1–C4 = 1.952(3), C3–O1 = 1.137(3), C4–O2 = 1.132(3); P1–Pd1–P2 = 88.19(2), C3–Pd1–C4 = 109.8(1), Pd1,P1,P2/Pd1,C3,C4 = 88.3(8).

longer than in TP-3 (R₂PC₂H₄PR₂)Pd⁰ complexes (2.30 Å, mean)^{11,12} and result from the different coordination geometry at Pd⁰. The Pd–CO bond distances average 1.946(8) Å and are longer than the corresponding bond in {MeC(CH₂PPh₂)₃}Pd(CO) (1.91 Å),^{1c} presumably as a result of the reduced back-bonding to two CO groups. In accord with this, the mean C–O bond length of 1.136(6) Å is almost identical to that of uncoordinated CO (1.13 Å).

Solid-State CP-MAS NMR Spectra of 2. Differences between the independent molecules of crystalline **2** are readily discernible in the ambient-temperature solid-state NMR spectra (Figure 2). The ¹³C CP-MAS spectrum displays four sharply resolved, closely positioned CO ligand resonances centered at $\delta(C)$ 198.2, which nicely agrees with the corresponding solution NMR shift ($\delta(C)$ 198.7). For the eight quaternary C atoms of the d⁴bpe ligands five signals (relative intensity 1:4:1:1:1) are observed, for which the mean chemical shift value of $\delta(C)$ 34.3 almost coincides with that for the solution ($\delta(C)$ 34.2). The ³¹P CP-MAS spectrum exhibits two signal groupings in the region of the isotropic chemical shift ($\delta(P)$ 83–77) consisting of four lines each. The fine-structure of the four lines at lower field depends on the rotation frequency, indicative of a spin–spin-coupled system. The analysis of the J-resolved 2D spectrum unequivocally reveals that the two signal groups represent independent {AB} spin systems with similar, but not identical, couplings.

Thus, both the ¹³C and the ³¹P CP-MAS chemical shifts are within narrow ranges and the differences from the solution NMR data are small. We conclude from these results that the structure of **2** (and presumably also that of **1**) in solution is the same as in the solid.

{(d⁴bpe)Pd}₂(μ -CO) (**3**). When solutions of the colorless mononuclear complexes **1** and **2** are concentrated

(10) Pörschke, K.-R.; Pluta, C.; Proft, B.; Lutz, F.; Krüger, C. Z. Naturforsch., B: Anorg. Chem., Org. Chem. **1993**, *48*, 608.

(11) (a) Krause, J.; Pluta, C.; Pörschke, K.-R.; Goddard, R. J. Chem. Soc., Chem. Commun. **1993**, 1254. Krause, J.; Haack, K.-J.; Pörschke, K.-R.; Gabor, B.; Goddard, R.; Pluta, C.; Seevogel, K. J. Am. Chem. Soc. **1996**, *118*, 804. (b) Goddard, R.; Hopp, G.; Jolly, P. W.; Krüger, C.; Mynott, R.; Wirtz, C. J. Organomet. Chem. **1995**, *486*, 163.

(12) Schager, F.; Bonrath, W.; Pörschke, K.-R.; Kessler, M.; Krüger, C.; Seevogel, K. Organometallics **1997**, *16*, 4276.

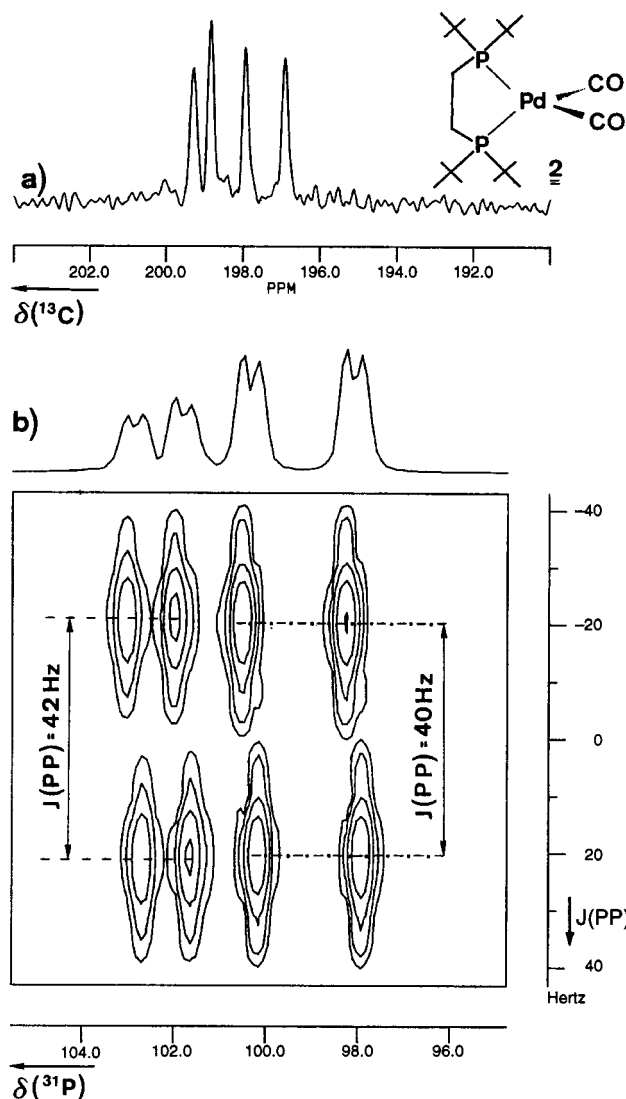


Figure 2. Solid-state CP-MAS NMR spectra of **2**: (a) ^{13}C CP-MAS NMR spectrum, showing four well-resolved carbonyl resonances for the two inequivalent molecules in the asymmetric unit, each of them having two CO ligands; (b) part of the J -resolved 2D ^{31}P CP-MAS NMR spectrum in the region of the first high-field rotation sideband. The two inequivalent molecules of **2** give rise to individual {AB} spin systems with different $J(\text{PP})$ coupling constants.

under vacuum, CO evolves and the solutions turn red. For the reaction of **1** a mixture of products is formed, of which only $\text{Pd}_2(\mu\text{-d}^4\text{ppe})_2$ ($\delta(\text{P})$ 33.7)^{12,13} has been identified (^{31}P NMR). From the reaction solution of **2** orange crystals of the dinuclear Pd^0 -monocarbonyl complex **3** separate at -30°C (Scheme 1). Solid **3** decomposes at 140°C (determined by DTA) and is thus more stable than the Pd^0 -dicarbonyl complexes **1** and **2**. In the EI mass spectrum (180°C), the molecular ion of $\text{Pd}(\text{tBu}_2\text{PC}_2\text{H}_4\text{P}(\text{O})\text{tBu}_2)_2$ (m/e 774, 5%) is found, resulting from partial phosphine oxidation and Pd elimination. The IR and solid-state and solution NMR spectra confirm the composition of **3** and are treated in more detail following a description of the molecular structure in the crystal.

(13) Schager, F.; Haack, K.-J.; Mynott, R.; Ruffínska, A.; Pörschke, K.-R. *Organometallics* **1998**, *17*, 807.

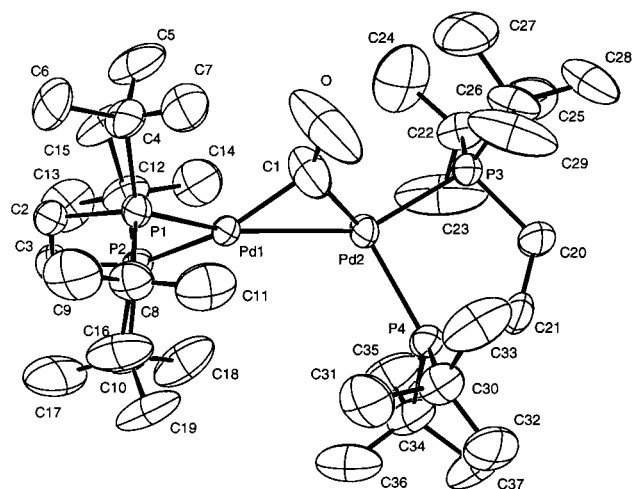


Figure 3. Molecular structure of complex **3**. Selected bond distances (Å) and bond angles and dihedral angles (deg): Pd1–Pd2 = 2.714(1), Pd1–C1 = 1.95(1), Pd2–C1 = 2.01(1), Pd1–P1 = 2.344(2), Pd1–P2 = 2.352(2), Pd2–P3 = 2.351(2), Pd2–P4 = 2.381(2), C1–O = 1.14(1); P1–Pd1–P2 = 90.0(1), P3–Pd2–P4 = 89.7(1), Pd1–C1–Pd2 = 86.3(4), P1–Pd1–C1 = 108.3(3), P2–Pd1–C1 = 149.6(5), P3–Pd2–C1 = 110.1(3), P4–Pd2–C1 = 142.6(5), Pd1, C1, O, Pd2/P1–P2, Pd1, Pd2 = 30(2), Pd1, C1, O, Pd2/P3, P4, Pd1, Pd2 = 44(2).

The solution NMR spectra are unchanged when MeOH is added to a solution of **3**. Notably, no Pd–H resonance is observed. Furthermore, no reaction occurs between **3** and H_2 at normal temperature and pressure. Complex **3** reacts quantitatively with CO to re-form **2**. Similarly, reaction with an excess of ethene affords the starting material (d^4bpe) $\text{Pd}(\text{C}_2\text{H}_4)$, and with ethyne (d^4bpe) $\text{Pd}(\text{C}_2\text{H}_2)$ is formed.

An approximately equimolar mixture of (d^4bpe) $\text{Pd}(\text{C}_2\text{H}_4)$ and the Pd^0 -dicarbonyl **2** displays a single broad resonance at $\delta(\text{P})$ 77.9 in its ambient-temperature ^{31}P NMR spectrum, indicating rapid CO exchange. When the solution is cooled to -80°C , this resonance splits into four sharp signals, which are attributable to major amounts of (d^4bpe) $\text{Pd}(\text{C}_2\text{H}_4)$ ($\delta(\text{P})$ 84.8) and **2** ($\delta(\text{P})$ 81.2) and minor amounts of the dinuclear Pd^0 -carbonyl **3** ($\delta(\text{P})$ 68.8) and CO-free **4'** ($\delta(\text{P})$ 72.1; see below). These results show that the formation of a stable mononuclear $\text{TP-3 L}_2\text{Pd}(\text{CO})$ ($\text{L}_2 = \text{d}^4\text{bpe}$) can be ruled out.

Molecular Structure of 3. The results of the crystal structure analysis of **3** are summarized in Figure 3. The complex exhibits approximate C_2 symmetry, with the major axis passing through the C–O vector and the center of the Pd1–Pd2 bond. The Pd1–Pd2 bond length at 2.714(1) Å is slightly shorter than that of palladium metal (2.745(2) Å) and is among the shortest found for Pd^0 complexes. The atoms Pd1, Pd2, P1, and P2 are approximately coplanar (plane 1, rms deviation 0.013 Å), and their mean plane makes an angle of $74(1)^\circ$ to the mean plane through the atoms Pd1, Pd2, P3, and P4 (plane 2, rms deviation 0.006 Å). The position adopted by the CO group is particularly worthy of note. Viewed along the Pd1–Pd2 axis, the CO group adopts a position approximately bisecting the *smaller* angle subtended by the two planes defined above, with the mean plane through the atoms Pd1, Pd2, C1, and O making an angle of $30(1)^\circ$ to plane 1 and $44(1)^\circ$ to plane

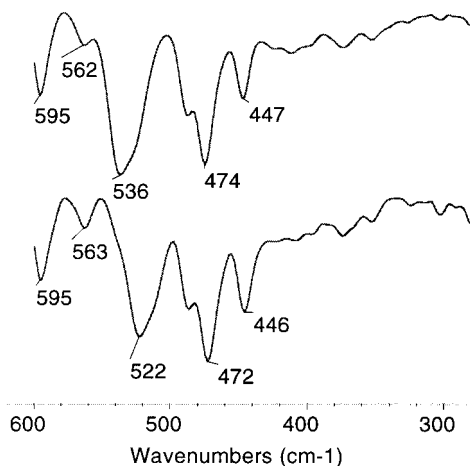


Figure 4. Far-IR transmittance spectra of PE-embedded **3** (top) and ^{13}CO -labeled **3** (bottom).

2. Thus, the CO group in **3** appears to take up a sterically less favored position.

The Pd-C bonds in **3** (1.98(4) Å (mean, libration corrected)) are slightly longer than those in *T*-4 **2** (1.95 Å), which contains terminally bound CO ligands but shorter than those observed for the higher Pd⁰-CO clusters. The C-O bond length of 1.14(1) Å (libration corrected, 1.15(1) Å) is nevertheless only slightly longer than the mean value observed for **2**. The four Pd-P bonds at 2.36(2) Å (mean) are shorter than those in *T*-4 **2** (Pd-P 2.41 Å), although still relatively long (cf. $(^n\text{Bu}_3\text{P})_4\text{Pd}_4(\mu_2\text{-CO})_6$: Pd-Pd, 2.79 Å; Pd-C, 2.06 Å; Pd-P, 2.26 Å).^{5b}

The structure of **3** is remarkably similar to that of the dinuclear Pd^I-carbonyl-hydride $[\{(\text{d}^1\text{ppp})\text{Pd}\}_2(\mu\text{-CO})(\mu\text{-H})]^+\text{Cl}^-$,¹⁴ in which Pd^I has a distorted-planar configuration. There was, however, no evidence of a bridging hydride ligand or a counterion in the crystal of **3**. Complex **3** is best described as a dinuclear Pd⁰ complex in which a necessarily weak d¹⁰-d¹⁰ Pd⁰-Pd⁰ bond is bridged by a strongly coordinating $\mu\text{-CO}$ ligand.

IR Spectra of 3. The IR spectrum of **3** shows a strong C-O stretching band at 1773 cm⁻¹ and a highly C-sensitive mode at 536 cm⁻¹, attributable to a strong Pd₂-($\mu\text{-CO}$) bridge and tentatively assigned to $\delta(\text{Pd-C-O}) + \gamma(\text{Pd-CO})$. The assignment has been made by comparison with the ^{13}CO -labeled isotopomer (1732, 522 cm⁻¹); no bands arise from the $\mu\text{-CO}$ ligand below 500 cm⁻¹ (Figure 4). The observed $^{12/13}\text{C}$ isotopic effect on the C-O stretching frequency is approximately 1.024. This ratio is in close agreement with the calculated value $(u'/u)^{1/2} = 1.023$ for uncoupled oscillating C-O, where u and u' are the reduced masses of ^{12}CO and ^{13}CO . The C-O stretching band is at markedly lower wavenumber than the corresponding bands for $(\text{Ph}_2\text{MeP})_4\text{Pd}_4(\mu_2\text{-CO})_5$ (1840/1820 cm⁻¹),^{5a} but it is not as low as for $(\text{Me}_3\text{P})_7\text{Pd}_6(\mu_3\text{-CO})_4$ ^{5c} (1730, 1708 cm⁻¹). The C-O and Pd-CO IR absorptions of **3** are considerably at variance with the data reported for CO adsorption on a Pd(100) surface (e.g. 1904 and 339 cm⁻¹),⁷ although the structural model suggested for the latter corresponds to the structure of **3**.^{7b}

(14) X-ray: Pd-Pd = 2.77 Å, Pd-C = 2.025 Å (mean); Pd-C-Pd = 86.2°, P-Pd-P = 126°; dihedral angle at Pd 16.2°. IR: $\nu(\text{CO})$ 1789 cm⁻¹, ^{13}C NMR: δ 250.9 (quint, $^2J(\text{PC}) = 32$ Hz, $\mu\text{-CO}$). Portnoy, M.; Frolow, F.; Milstein, D. *Organometallics* **1991**, *10*, 3960.

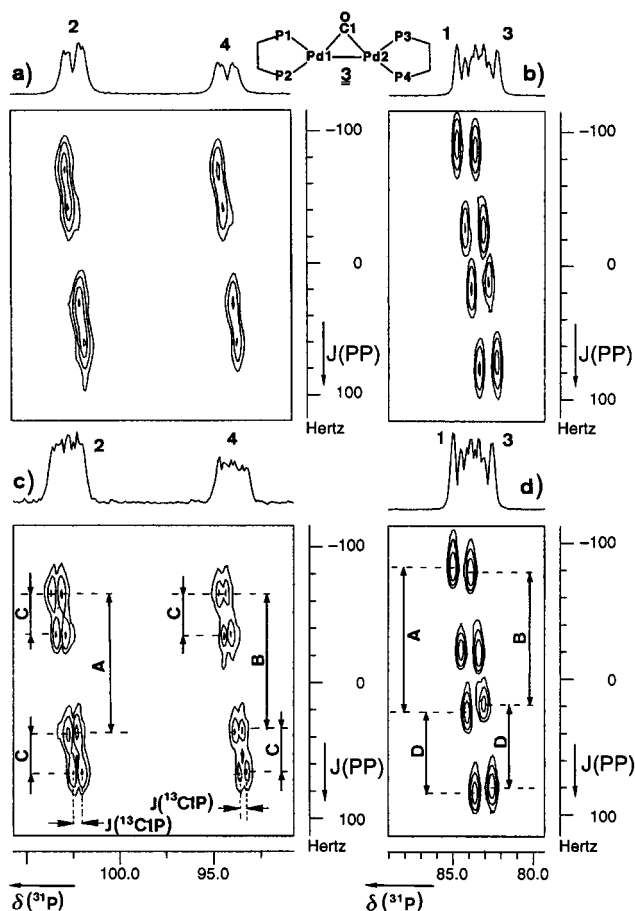


Figure 5. Parts of the solid-state J -resolved 2D ^{31}P CP-MAS NMR spectra of unlabeled **3** (a,b) and ^{13}CO -labeled **3** (c,d) in the region of the first high-field rotation sidebands. (c) In the F2 dimension the signals of P2 and P4 display $^2J(\text{PC})$ heterocouplings to the ^{13}CO ligand. (c,d) The $J(\text{PP})$ couplings, observable in the F1 dimension, are $A = 105 \pm 5$ Hz, $B = 98 \pm 5$ Hz, $C = 32 \pm 5$ Hz, and $D = 60 \pm 5$ Hz.

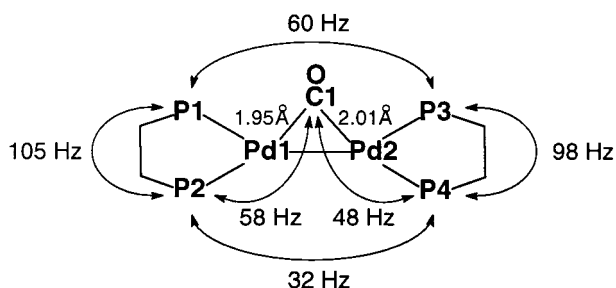
Solid-State and Solution NMR Spectra of 3. The solid-state NMR spectra of **3** are rather complex, unlike the relatively simple spectra of **2**. In the ^{31}P CP-MAS NMR spectrum of ^{13}CO -labeled **3**, two multiplets at $\delta(\text{P})$ 77.0 (relative intensity 1P) and 68.4 (1P) and two strongly overlapping multiplets centered at $\delta(\text{P})$ 58.1 (2P) are observed, the isotropic range thereby spanning 20 ppm. The fine structure of these signals changes only marginally when the rotation frequency is altered (1.5–5 kHz). The spectrum of unlabeled **3** is very similar, but in particular, the lines of the two low-field multiplets are somewhat better resolved. The spectra are temperature-independent between 24 and 57 °C.

Analysis of the J -resolved 2D ^{31}P NMR spectrum (Figure 5) reveals that the splitting of the low-field multiplets of the ^{13}CO -labeled compound is attributable to cross-peaks in both the F1 (scalar $J(\text{PP})$ couplings) and F2 dimensions (chemical shifts). The F2 cross-peaks are absent in the spectrum of the unlabeled compound, which clearly shows that the corresponding coupling is due to the ^{13}C nucleus of the CO ligand. The high-field multiplet represents a pair of double doublets at $\delta(\text{P})$ 58.6 ($J(\text{PP}) = 105$ and 60 Hz) and 57.6 ($J(\text{PP}) = 98$ and 60 Hz) (accuracy of all couplings ± 5 Hz). Comparison of the line width of these resonances for the ^{13}CO -labeled

and unlabeled compounds indicates that $^2J(\text{PC})$ couplings are either small or even not present.

These results can be correlated with the X-ray structural data of **3**. The two Pd–CO bonds are different (1.95, 2.01 Å), and so are the corresponding four P–Pd–C angles (108–150°) (see Figure 3), allowing an assignment of the ^{31}P resonances to the individual P atoms. The signal at $\delta(\text{P})$ 77.0 ($J(\text{P2P1}) = 105$ Hz, $^3J(\text{P2P4}) = 32$ Hz), for which $^2J(\text{PC}) = 58$ Hz is largest, is attributed to P2 at Pd1, because the angle P2–Pd1–C1 (150°) is closest to trans and the Pd1–C1 bond is short, allowing strong $^2J(\text{PC})$ coupling. Accordingly, the signal at $\delta(\text{P})$ 68.4 ($J(\text{P4P3}) = 98$ Hz, $^3J(\text{P4P2}) = 32$ Hz) with a coupling nearly as large, $^2J(\text{PC}) = 48$ Hz, is assigned to P4 at Pd2 because of the still large angle P4–Pd2–C1 (143°) and the now longer bond Pd2–C1. The assignment of the further resonances to P1 and P3 is based on the fact that for electron-rich ($\text{d}^{\text{bpe}}\text{M}^0$) chelate complexes $J(\text{PP})$ couplings can be as large as >100 Hz.¹⁵ Consequently, the signal at $\delta(\text{P})$ 58.6 is ascribed to P1 at Pd1 and that at $\delta(\text{P})$ 57.6 to P3 at Pd2.

Hence, the smaller but still significant couplings of 60 and 32 Hz are due to couplings between the ^{31}P nuclei of different d^{bpe} ligands. The magnitude of these couplings can only be explained by $^3J(\text{PP})$ couplings transmitted by a Pd–Pd bond, because possible $^4J(\text{PP})$ couplings (via P–Pd–C–Pd–P) are expected to be much smaller. Inspection of the torsional angle values between the individual P atoms reveals that P1–Pd1–Pd2–P3 (–70.3°) and P2–Pd1–Pd2–P4 (–75.6°) are relatively small, whereas P1–Pd1–Pd2–P4 (+108.0°) and P2–Pd1–Pd2–P3 (+106.2°) are markedly larger. Assuming that a Karplus-type relationship is valid for $^3J(\text{PP})$ couplings, similar to what has been established for $^3J(\text{PC})$,¹⁶ distinct $^3J(\text{PP})$ couplings should be observable for the ^{31}P nuclei at torsional angles of about 70° but not for those at about 110°. These considerations are in agreement with the experimentally found couplings $^3J(\text{P1P3}) = 60$ Hz, $^3J(\text{P2P4}) = 32$ Hz,^{17a} and $^3J(\text{P1P4}) \approx ^3J(\text{P2P3}) \approx 0$.



Thus, characteristics of the solid-state ^{31}P NMR spectra of **3** are, in particular, (i) the large differences in the chemical shifts of the individual ^{31}P nuclei ($\delta(\text{P})$ 77.0–57.6; mean 65.4), (ii) pronounced $^3J(\text{PC})$ couplings

(15) Bach, I.; Pörschke, K.-R.; Goddard, R.; Kopiske, C.; Krüger, C.; Rufiniska, A.; Seevogel, K. *Organometallics* **1996**, *15*, 4959.

(16) Quin, L. D. In *Phosphorus-31 NMR Spectroscopy in Stereochemical Analysis*; Verkade, J. G., Quin, L. D., Eds.; VCH: Deerfield, FL, 1987; p 392f.

(17) (a) For $\{(\text{tBu}_2\text{PC}_3\text{H}_6\text{P}^i\text{Bu}_2)\text{Pt}\}_2$ (P–Pt–Pt–P = 82°) the coupling $^3J(\text{PP}) = 30$ Hz was found in solution.^{17c} (b) Complex **4** is related to the structurally characterized $\{(\text{tBu}_2\text{PC}_3\text{H}_6\text{P}^i\text{Bu}_2)\text{Pt}\}_2$.^{17c} (c) Yoshida, T.; Yamagata, T.; Tulip, T. H.; Ibers, J. A.; Otsuka, S. *J. Am. Chem. Soc.* **1978**, *100*, 2063. Dedieu, A.; Hoffmann, R. *J. Am. Chem. Soc.* **1978**, *100*, 2074.

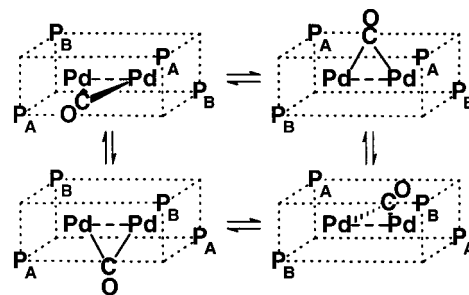


Figure 6. Suggested mechanism for the structural dynamics of **3** in solution. P_A and P_B denote inequivalent, mean positions of the “wobbling” phosphorus atoms while the CO ligand precesses about the Pd...Pd axis. Exchange of P_A and P_B leads to an equilibration of the ^{31}P nuclei.

to the CO ligand for *two* of the four ^{31}P nuclei in the solid state, (iii) strong $^3J(\text{PP})$ couplings between the different d^{bpe} ligands, and (iv) the temperature independence of the solid-state NMR spectra. These features are in agreement with a rigid structure and an intact Pd–Pd bond of **3** in the solid state, as has also been shown by the X-ray analysis.

In contrast to the solid-state spectra, the solution ^1H , ^{13}C , and ^{31}P NMR spectra (27 °C) of **3** are rather simple. For the μ -CO ligand ^{13}C -enriched **3** exhibits a low-field A_4X quintet at $\delta(\text{C})$ 243.5, with the averaged coupling $^2J(\text{PC}) = 23.3$ Hz. The resonances for the d^{bpe} ligands indicate that both ($\text{d}^{\text{bpe}}\text{Pd}$) moieties are equivalent and have local C_{2v} symmetry. In the ^{31}P NMR spectrum a sharp singlet at $\delta(\text{P})$ 68.8 is found which is split into a doublet for the ^{13}C isotopomer, confirming that only one CO ligand is present. No line-broadening of either the ^{31}P singlet or the ^{13}C quintet of **3** is observed at –80 °C.

Considering the lower symmetry of the complex in the solid state, it can be concluded that the structure of **3** is dynamic in solution, leading to an equilibration of all the P atoms, and that the activation energy for the rearrangement is very low. To explain the structural dynamics, we exclude any rotation of the bulky ($\text{d}^{\text{bpe}}\text{Pd}$) moieties against each other in view of the presumed steric hindrance and the ease with which the dynamics occur, even at low temperature. However, the differences in the solid-state and solution NMR spectra suggest a marked change in the structure of **3**. This change seems best to be explained by considerable weakening or even cleavage of the Pd⁰–Pd⁰ bond, thus allowing the CO ligand to precess inside a more or less stationary $\text{P}_2\text{Pd}\cdots\text{PdP}_2$ skeleton as depicted in Figure 6.¹⁸

{(d^{bpe}Pd)}₂ (4). When solutions of **3** are kept at ambient temperature, the CO ligand is eliminated and beige, insoluble **4** precipitates. The reaction is markedly faster in THF (half-time 1 day) than in toluene (half-time 4 days). Monitoring the reaction by NMR reveals new weak NMR signals, close to those of residual **3**. The same resonances without further splitting are observed when **4** is prepared from ^{13}C -enriched **3**. We attribute these resonances, in particular a sharp ^{31}P NMR singlet

(18) A related mechanism has been suggested for the structural dynamics of $\{(\text{d}^{\text{bpe}}\text{Ni})_2(\mu\text{-H})_2\}$: Bach, I.; Goddard, R.; Kopiske, C.; Seevogel, K.; Pörschke, K.-R. *Organometallics* **1999**, *18*, 10.

at $\delta(\text{P})$ 72.1,¹⁹ to **4'** (possibly monomeric "(d^bbpe)Pd") as a soluble precursor complex to the insoluble **4**, for which neither solution NMR spectra nor reliable solid-state NMR spectra have been obtainable. In the IR spectrum of **4** no bands appear between 2800 and 1500 cm⁻¹, ruling out the presence of coordinated CO. Isolated **4** decomposes only above 260 °C. The EI mass spectrum of **4** displays a weak M⁺ peak at *m/e* 848 and thus differs principally from that of **3**. Although isolated **4** is virtually insoluble, it dissolves upon reaction with an excess of ethene, ethyne (both in the course of a few minutes), and CO (instantly) to give starting (d^bbpe)-Pd(C₂H₄), (d^bbpe)Pd(C₂H₂),⁹ and **2**, respectively (Scheme 1). Complex **4** appears to be an oligomer of (d^bbpe)Pd⁰ moieties with chelating d^bbpe ligands, and we tentatively assume it to be a roughly D_{2d} symmetrical dimer with an unsupported Pd⁰–Pd⁰ d¹⁰–d¹⁰ bond that is shielded by the eight *tert*-butyl substituents.^{17b}

Conclusions

Complexes **1** and **2** are the first isolated Pd⁰–dicarbonyl complexes. They demonstrate that the homologous series L₂M(CO)₂ is accessible for M = Ni, Pd, Pt, even though the Pd complexes are markedly less stable than their Ni and Pt analogues. In solution, the CO ligands of **1** and **2** are readily displaced by other π -ligands, the reactivity of **1** and **2** being comparable with that of the Pd⁰–ethene complexes, from which they are prepared in equilibrium reactions.

Partial CO cleavage from **2** gives rise to dinuclear **3**, in which the Pd atoms are singly bridged by CO. Complex **3** represents the lowest member of a series of L_{*n*}Pd_{*x*}(μ_2 -CO)_{*y*} cluster compounds. It also serves as a model for the adsorption of CO on a Pd metal surface, since Pd₂(μ -CO) coordination has been suggested.

It appears that for the Pd⁰–CO system the Pd₂(μ -CO) entity is strongly favored over other possible coordination modes (e.g., Pd– σ -CO and Pd₂(μ -CO)₂).

Experimental Section

To exclude oxygen and moisture, all operations were conducted under an atmosphere of argon by standard Schlenk techniques. Details of the spectroscopic instruments¹³ and solid-state CP-MAS NMR spectroscopy¹⁵ are described elsewhere. For solution NMR spectra THF-*d*₈ was used if not indicated otherwise. ¹³CO gas (99% isotopic purity; 10% ¹³C¹⁸O) was obtained from Cambridge Isotope Laboratories, Andover, MA.

(ⁱPr₂PC₂H₄PⁱPr₂)Pd(CO)₂ (1**).** A colorless solution of (dⁱppe)-Pd(C₂H₄) (397 mg, 1.00 mmol) in pentane (5 mL) was treated with CO at 20 °C. The solution instantaneously turned light red and eventually beige (after 2 min). At –78 °C colorless crystals separated, from which the mother liquor was removed by cannulation. The solid was washed with cold pentane and dried under vacuum at –30 °C (causing a superficial tinge of yellow): yield 310 mg (73%); dec pt 42 °C. IR (pentane): 2016 ($\nu_{\text{sym}}(\text{CO})_2$), 1978 cm⁻¹ ($\nu_{\text{as}}(\text{CO})_2$). ¹H NMR (200 MHz, 27 °C): δ 1.92 (m, 4H, PCH), 1.58 (m, 4H, PCH₂), 1.12, 1.06 (each m, 12H, Me), dⁱppe. ¹³C NMR (75.5 MHz, –80 °C): δ 199.0 (t, ²*J*(PC) = 4 Hz), CO; 25.5 ("t", 4C, PCH), 22.7 ("t", 2C, PCH₂), 19.8 ("t"), 18.2 ("s", each 4C, Me), dⁱppe. ³¹P NMR (81 MHz, 27

°C): δ 59.5. Anal. Calcd for C₁₆H₃₂O₂P₂Pd (424.8): C, 45.24; H, 7.59; O, 7.53; P, 14.58; Pd, 25.05. Found: C, 45.21; H, 7.54; P, 14.72.

(^tBu₂PC₂H₄P^tBu₂)Pd(CO)₂ (2**).** The synthesis was similar to that for **1** in that (d^bbpe)Pd(C₂H₄) (453 mg, 1.00 mmol) was reacted with CO in pentane at 20 °C: colorless cubes; yield 390 mg (81%); mp 125 °C dec. IR (KBr): 1990 ($\nu_{\text{sym}}(\text{CO})_2$), 1947 cm⁻¹ ($\nu_{\text{as}}(\text{CO})_2$). IR (pentane): 2012 ($\nu_{\text{sym}}(\text{CO})_2$), 1969 cm⁻¹ ($\nu_{\text{as}}(\text{CO})_2$). ¹H NMR (300 MHz, 27 °C): δ 1.74 (m, 4H, PCH₂), 1.22 (m, 36H, Me), d^bbpe. ¹³C NMR (75.5 MHz, –80 °C): δ 198.7 (t, ²*J*(PC) = 4.5 Hz), CO; 34.2 ("s", 4C, PC), 30.0 ("t", 12C, Me), 24.3 ("t", 2C, PCH₂), d^bbpe. ³¹P NMR (81 MHz, 27 °C): δ 81.2. Anal. Calcd for C₂₀H₄₀O₂P₂Pd (480.9): C, 49.95; H, 8.38; O, 6.65; P, 12.88; Pd, 22.13. Found: C, 49.65; H, 8.55; P, 13.15. ¹³C CP-MAS (24 °C): δ 199.3 (1C), 198.8 (1C), 197.9 (1C), 196.9 (1C), all s, CO; 35.0 (1C), 34.6 (4C), 34.2 (1C), 33.8 (1C), 33.3 (1C), all s, PC; 31.5–30.4 (several lines of variable intensities), CMe; 24.8 (broad, unresolved line), PCH₂. ³¹P CP-MAS (24 °C): δ 82.8, 81.6 (each 1P, *J*(PP) = 42 ± 5 Hz), d^bbpe of molecule 1; 80.2, 77.9 (each 1P, *J*(PP) = 40 ± 5 Hz), d^bbpe of molecule 2.

{(^tBu₂PC₂H₄P^tBu₂)Pd}₂(μ -CO) (3**).** A solution of **2** (481 mg, 1.00 mmol) in pentane (5 mL) was evaporated to dryness under vacuum. The red residue was dissolved in pentane (10 mL), and the solution was filtered to remove some insoluble impurities. When the filtrate was cooled to –30 °C, orange cubes separated, which were isolated as described above: yield 280 mg (62%); dec pt 140 °C. IR (KBr): see text. ¹H NMR (200 MHz, 27 °C): δ 1.76 (m, 8H, PCH₂), 1.25 (m, 72H, Me), d^bbpe. ¹³C NMR (75.5 MHz, 27 °C): δ 243.5 (quint, ²*J*(PC) = 23.3 Hz), μ -C≡O; 35.0 ("s", 8C, PC), 31.3 ("t", 24C, Me), 23.9 ("t", 4C, PCH₂), d^bbpe. ³¹P NMR (81 MHz, 27 °C): δ 68.8. Anal. Calcd for C₃₇H₈₀OP₄Pd₂ (877.8): C, 50.63; H, 9.19; O, 1.82; P, 14.11; Pd, 24.25. Found: C, 50.49; H, 9.28; P, 14.26; Pd, 24.19. ¹³C CP-MAS NMR (24 °C): δ 245.0 ("t", Σ *J*(PC1) = 72 Hz), μ -CO; 36.0 (2C), 35.6 (2C), 35.2 (1C), 34.6 (1C), 34.2 (2C), PC; 33–30 (several lines of different intensities), Me; 25.2, 22.6 (each broad m), PCH₂. ³¹P CP-MAS NMR (24 °C) (for the designation of ³¹P nuclei, see Figure 3): δ 77.0 (m, *J*(P2P1) = 105 ± 5 Hz, ³*J*(P2P4) = 32 ± 5 Hz, ²*J*(P2C1) = 58 ± 5 Hz), P2; 68.4 (m, *J*(P4P3) = 98 ± 5 Hz, ³*J*(P4P2) = 32 ± 5 Hz, ²*J*(P4C1) = 48 ± 5 Hz), P4; 58.6 (m, *J*(P1P2) = 105 ± 5 Hz, ³*J*(P1P3) = 60 ± 5 Hz, ²*J*(P1C1) ≈ 0 Hz), P1; 57.6 (m, *J*(P3P4) = 98 ± 5 Hz, ³*J*(P3P1) = 60 ± 5 Hz, *J*(P3C1) ≈ 0 Hz), P3.

{(^tBu₂PC₂H₄P^tBu₂)Pd}₂ (4**).** A red solution of **3** (878 mg, 1.00 mmol) in toluene (10 mL) was stirred at 70 °C for 6 h. The color of the solution lightened markedly, and a beige precipitate was obtained, which was isolated by filtration, washed with pentane, and dried under vacuum (20 °C): yield 340 mg (40%); dec pt >260 °C. For the isolated compound neither solution NMR nor meaningful solid-state ¹³C and ³¹P CP-MAS NMR spectra have been obtained. Anal. Calcd for C₃₆H₈₀P₄Pd₂ (849.8): C, 50.88; H, 9.49; P, 14.58; Pd, 25.05. Found: C, 51.03; H, 9.42; P, 14.46; Pd, 25.10.

Crystal Structure Determination of **2:** C₂₀H₄₀O₂P₂Pd, *M_r* = 480.86, colorless (superficially red-brown), crystal size 0.39 × 0.21 × 0.53 mm, *a* = 11.3822(5) Å, *b* = 17.1554(7) Å, *c* = 24.555(1) Å, β = 90.063(2)°, *U* = 4794.5(3) Å³, *T* = 100 K, monoclinic, *P*2₁/*c* (No. 14), *Z* = 8, *d*_{calcd} = 1.33 g cm⁻³, μ = 0.918 mm⁻¹, Siemens SMART diffractometer, λ = 0.710 73 Å, CCD ω -scan, 55 219 reflections, 17 877 independent, 11 472 observed (*I* > 2 σ (*I*)), [(sin θ)/ λ]_{max} = 0.79 Å⁻¹, analytical absorption correction (*T*_{min} = 0.567 14; *T*_{max} = 0.705 07), direct methods (SHELXS-97),²⁰ a least-squares refinement on *F*_o² (SHELXL-97),^{20b} H atoms riding, 451 refined parameters, *R* = 0.044 (observed data), *R_w* = 0.102 (Chebyshev weights), final shift/error 0.001, residual electron density 1.523 e Å⁻³ (0.823 Å from Pd1).

(19) ¹H NMR (200 MHz, toluene-*d*₈, 27 °C): δ 1.40 (m, 8H, PCH₂), 1.10 (m, 72H, Me), d^bbpe.

(20) (a) Sheldrick, G. M. *Acta Crystallogr., Sect. A* **1990**, *46*, 467. (b) Sheldrick, G. M. University of Göttingen, Göttingen, Germany, 1997.

Crystal Structure Determination of 3: $C_{37}H_{80}OP_4Pd_2$, $M_r = 877.69$, orange, crystal size $0.20 \times 0.48 \times 0.48$ mm, $a = 12.283(3)$ Å, $b = 16.388(3)$ Å, $c = 22.853(5)$ Å, $\beta = 104.94(3)^\circ$, $U = 4444.6(16)$ Å³, $T = 293$ K, monoclinic, $P2_1/n$ (No. 14), $Z = 4$, $d_{\text{calcd}} = 1.31$ g cm⁻³, $\mu = 0.978$ mm⁻¹, Nonius KappaCCD diffractometer, $\lambda = 0.71073$ Å, CCD ω -scan, 48 365 reflections, 10 068 independent, 8728 observed ($I > 2\sigma(I)$), $[(\sin \theta)/\lambda]_{\text{max}} = 0.65$ Å⁻¹, analytical absorption correction ($T_{\text{max}} = 0.83130$; $T_{\text{min}} = 0.60276$), direct methods (SHELXS-97),²⁰ least-squares refinement on F_o^2 (SHELXL-97),^{20b} H atoms riding, 397 refined parameters, $R = 0.069$ (observed data), $R_w = 0.173$ (Chebyshev

weights), final shift/error 0.001, residual electron density 1.477 e Å⁻³ (0.916 Å from Pd1).

Acknowledgment. We thank the Fonds der Chemischen Industrie for financial support.

Supporting Information Available: Tables of X-ray data collection information, atom coordinates and thermal parameters, and bond lengths and angles for **2** and **3**. This material is available free of charge via the Internet at <http://pubs.acs.org>. OM990239S